

Mutual optical injection in coupled DBR laser pairs

M.P. Vaughan¹, I. Henning^{1,*}, M.J. Adams¹, L.J. Rivers², P. Cannard² and I.F. Lealman²

¹*School of Computer Science and Electronic Engineering, University of Essex, Colchester CO4 3SQ*

²*CIP Technologies, Adastral Park, Ipswich, IP5 3RE*

*Corresponding author: idhem@essex.ac.uk

Abstract: We report an experimental study of nonlinear effects, characteristic of mutual optical coupling, in an ultra-short coupling regime observed in a distributed Bragg reflector laser pair fabricated on the same chip. Optical feedback is amplified via a double pass through a common on-chip optical amplifier, which introduces further nonlinear phenomena. Optical coupling has been introduced via back reflection from a cleaved-ended fibre. The coupling may be varied in strength by varying the distance of the fibre from the output of the chip, without significantly affecting the coupling time.

©2008 Optical Society of America

OCIS codes: (140.5960) Lasers and laser optics : Semiconductor lasers; (140.1540) Lasers and laser optics : Chaos; (190.4360) Nonlinear optics : Nonlinear optics, devices; (190.5970) Nonlinear optics : Semiconductor nonlinear optics including MQW; (250.5960) Optoelectronics : Semiconductor lasers; (250.4390) Optoelectronics : Nonlinear optics, integrated optics.

References and links

1. J. M. Buldu, R. Vicente, T. Perez, C. R. Mirasso, M. C. Torrent, and J. Garcia-Ojalvo "Periodic entrainment of power dropouts in mutually coupled semiconductor lasers," *Appl. Phys. Lett.* **81**, 5105-5107 (2002).
2. J. Mulet, C. Masoller, and C. R. Mirasso, "Modeling bidirectionally coupled single-mode semiconductor lasers," *Phys. Rev. A* **65**, 063815 (2002).
3. J. Revuelta, C. R. Mirasso, P. Colet, and L. Pesquera, "Criteria for synchronization of coupled chaotic external-cavity semiconductor lasers," *IEEE Photon. Technol. Lett.* **14**, 140-142 (2002).
4. C. R. Mirasso, M. Kolesik, M. Matus, J. K. White, and J. V. Moloney, "Synchronization and multimode dynamics of mutually coupled semiconductor lasers," *Phys. Rev. A* **65**, 013805 (2002).
5. F. Rogister and J. Garcia-Ojalvo, "Symmetry breaking and high-frequency periodic oscillations in mutually coupled laser diodes," *Opt. Lett.*, **28**, 1176 (2003).
6. R. Vicente, J. Mulet, M. Sciamanna, and C. R. Mirasso, "Simple interpretation of the dynamics of mutually coupled semiconductor lasers with detuning," *Proc. SPIE* **5349**, 307 (2004).
7. R. Vicente, S. Tang, J. Mulet, C.R. Mirasso, and J.M. Liu, "Dynamics of semiconductor lasers with bidirectional optoelectronic coupling: Stability, route to chaos, and entrainment," *Phys. Rev. E* **70**, 046216 (2004).
8. S. Tang, R. Vicente, M. C. Chiang, C. R. Mirasso, and J. M. Liu, "Nonlinear dynamics of semiconductor lasers with mutual optoelectronic coupling," *IEEE J. Sel. Top. Quantum Electron.* **10**, 936-943 (2004).
9. S. Wiczorek and W. W. Chow, "Bifurcations and interacting modes in coupled lasers: A strong-coupling theory," *Phys. Rev. A* **69**, 033811 (2004).
10. J. Mulet, C. Mirasso, T. Heil, and I. Fischer, "Synchronization scenario of two distant mutually coupled semiconductor lasers," *J. Opt. B: Quantum Semiclass. Opt.* **6**, 97-105 (2004).
11. T. Perez, M. Radziunas, H. J. Wunsche, C. R. Mirasso, and F. Henneberger, "Synchronization properties of two coupled multisection semiconductor lasers emitting chaotic light," *IEEE Photon. Technol. Lett.* **18**, 2135-2137 (2006).
12. X. Li, W. Pan, B. Luo and D. Ma, "Nonlinear dynamics of two mutually injected external-cavity semiconductor lasers" *Semicond. Sci. Technol.* **21**, 25 (2006).
13. J.F. Avila, R. Vicente, J.R. Leite and C.R. Mirasso, "Synchronization properties of bidirectionally coupled semiconductor lasers under asymmetric operating conditions," *Phys. Rev. E* **75**, 066202 (2007).
14. R. Vicente, C. R. Mirasso, and I. Fischer, "Simultaneous bidirectional message transmission in a chaos-based communication scheme," *Opt. Lett.* **32**, 403-405 (2007).
15. B. Krauskopf and H. Erzgraber, "Delay-coupled semiconductor lasers near locking: a bifurcation study," (2008), <http://hdl.handle.net/1983/1073> (accessed Aug 2008).

16. A. Hohl, A. Gavrielides, T. Erneux, and V. Kovanis, "Localised synchronisation in two coupled nonidentical semiconductor lasers," *Phys. Rev. Lett.* **78**, 4745 (1997).
 17. T. Heil, I. Fischer, W. Elsasser, J. Mulet, and C. R. Mirasso, "Chaos synchronization and spontaneous symmetry-breaking in symmetrically delay-coupled semiconductor lasers," *Phys. Rev. Lett.* **86**, 795 (2001).
 18. N. Fujiwara, Y. Takiguchi, and J. Ohtsubo, "Observation of the synchronization of chaos in mutually injected vertical-cavity surface-emitting semiconductor lasers," *Opt. Lett.* **28**, 1677 (2003).
 19. R. Vicente, J. Mulet, C.R. Mirasso, and M. Sciamanna, "Bistable polarization switching in mutually coupled vertical-cavity surface-emitting lasers," *Opt. Lett.* **31**, 996-998 (2006).
 20. X.F. Li, W. Pan, B. Luo, D. Ma, and W. Zhang, "Nonlinear dynamics and localized synchronization in mutually coupled VCSELS," *Opt. Laser Technol.* **39**, 875-880 (2007).
 21. W. L. Zhang, W. Pan, B. Luo, X. F. Li, X. H. Zou, and M. Y. Wang, "Polarization switching of mutually coupled vertical-cavity surface-emitting lasers," *J Opt. Soc. Am. B* **24**, 1276-1282 (2007).
 22. W. L. Zhang, W. Pan, B. Luo, X. F. Li, X. H. Zou, and M. Y. Wang, "Polarization switching and synchronization of mutually coupled vertical-cavity surface-emitting semiconductor lasers," *Chin. Phys.* **16**, 1996-2002 (2007).
 23. W. L. Zhang, W. Pan, B. Luo, M. Y. Wang, and X. H. Zou, "Mode hopping and polarization switching of mutually coupled vertical-cavity surface-emitting lasers," *Sci. China Ser. F* **51**, 592-598 (2008).
 24. N. Jiang, W. Pan, B. Luo, W. Zhang, and D. Zheng, "Stable anticipation synchronization in mutually coupled vertical-cavity surface-emitting lasers system," *Chin. Opt. Lett.* **6**, 517-519 (2008).
 25. S. P. Hegarty, D. Goulding, B. Kelleher, G. Huyet, M. Todaro, A. Salhi, A. Passaseo, and M. De Vittorio, "Phase-locked mutually coupled 1.3 μm quantum-dot lasers," *Opt. Lett.* **32**, 3245 (2007).
 26. E. Wille, M. Peil, I. Fischer, and W. Elsasser, "Dynamical scenarios of mutually delay-coupled semiconductor lasers in the short coupling regime," *Proc. SPIE* **5452**, 41 (2004).
 27. H. Erzgraber, D. Lenstra, B. Krauskopf, E. Wille, M. Peil, I. Fischer, and W. Elsasser, "Mutually delay-coupled semiconductor lasers: Mode bifurcation scenarios," *Opt. Commun.* **255**, 286 (2005).
 28. A. E. Kelly, I. F. Lealman, L.J. Rivers, S.D. Perrin, and M. Silver, "Polarisation insensitive, 25dB gain semiconductor laser amplifier without antireflection coatings," *Electron. Lett.* **32**, 1835-1836 (1996).
 29. M. C. Tatham, G. Sherlock, and L. D. Westbrook, "20-nm optical wavelength conversion using nondegenerate 4-wave-mixing," *IEEE Photon. Technol. Lett.* **5**, 1303-1306 (1993).
 30. S. Diez, C. Schmidt, R. Ludwig, H. G. Weber, K. Obermann, S. Kindt, I. Koltchanov, and K. Petermann, "Four-wave mixing in semiconductor optical amplifiers for frequency conversion and fast optical switching," *IEEE J. Sel. Top. Quantum Electron.* **3**, 1131-1145 (1997)
-

1. Introduction

The dynamics of mutually coupled lasers are of considerable interest due to their potential application in laser diode arrays, noise reduction and frequency stabilisation in the phase-locking regime, and cryptographic applications based on chaotic communications. Moreover, the study of delay-coupled oscillators of itself has wide application in diverse areas of nonlinear dynamics, such as neural networks or population dynamics.

Mutually coupled lasers have been modelled theoretically [1-15] via coupled nonlinear differential equations for the carrier density, electric field amplitude and phase, where, in addition to the normal parameters found in laser rate equations, coupling strength, coupling time τ and, in some cases [12], optical feedback strength and feedback delay, are introduced. Comparison of $1/\tau$ with the relaxation oscillation frequencies ω_{RO} of the lasers allows mutually coupled systems to be classified into long and short coupling regimes. Most experimental investigations have been with the lasers in a face-to-face configuration with a separation of several centimetres so that τ is of the order of nanoseconds. Hence, $1/\tau$ is significantly less than ω_{RO} and these systems may be described as being in the long coupling regime. Such studies have yielded observations of localised and chaos synchronisation in edge-emitting lasers (EELS) [16, 17], vertical cavity surface emitting lasers (VCSELS) [18-24] and phase-locking in quantum dot (QD) lasers [25]. Studies of coupled distributed feedback (DFB) lasers in the short coupling regime ($\tau = 170$ ps) have also been undertaken [26, 27].

In the present study, we report observations of wavelength selection and nonlinear dynamics in twin distributed Bragg reflector (DBR) lasers fabricated on the same chip and coupled into a common semiconductor optical amplifier (SOA). The coupling time τ is of the order of tens of picoseconds, with $1/\tau$ much larger than the relaxation oscillation frequencies of the lasers and so may be described as being in the ultra-short coupling regime. This is in

contrast to end-to-end coupling schemes such as refs [14, 17] where the coupling time is much larger than the laser internal time scales. Moreover, in the present work the DBR laser pairs are non-identical, having been fabricated to obtain offset lasing wavelengths. Synchronised dynamics such as those reported in ref [17] in which the laser intensities follow each other lagging only by the coupling time might therefore not be expected in the current system. An additional degree of freedom not previously modelled or investigated to our knowledge is that the feedback and coupling is amplified via an integrated SOA, which also introduces additional nonlinear phenomena such as four-wave mixing.

2. Description of device

The device consists of two four-section DBR lasers fabricated side-by-side on the same chip using a buried heterostructure (BH) structure. The spacing between the adjacent laser cavities is wide enough to avoid any lateral coupling between the devices via their evanescent fields. Each laser has a long rear grating and a short front grating section with an intra cavity 100 μm long phase section and a 400 μm gain section (Fig. 1). The optical output from each laser is combined in a multi-mode interferometer (MMI) section and passes through a common SOA. The output waveguide is tapered to enlarge the spot size and angled to the device facet [28], which is further AR coated to minimise reflections. It is estimated that this approach leads to a residual reflectivity of $<10^{-5}$. From the chip dimensions, and defining the coupling time τ as the time it takes for light from the gain section of one laser to reach that of the other (i.e. reflected via the front facet) gives a value of $\tau \approx 30$ ps.

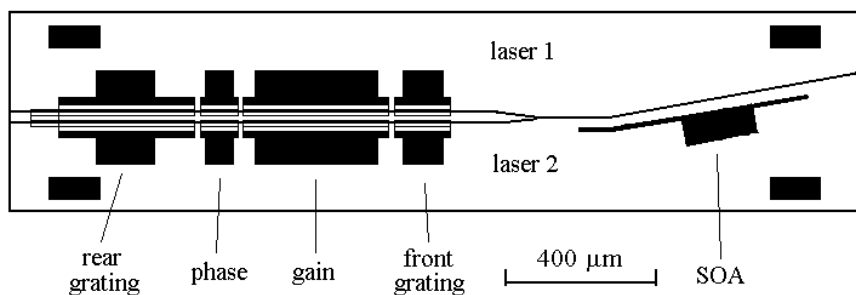


Fig. 1. Schematic of the twin DBR device showing contacts and waveguide. The solid black regions are the metal contacts over the laser sections (to scale).

In this section, we describe the characteristics of the uncoupled lasers operating individually. Initial free space measurements showed that with the SOA current set at 200 mA, the optical power output saturates at 35 mW – 40 mW as the laser gain currents were swept. Both lasers showed threshold currents of around 20 mA. With the gain current for each laser set at 100 mA, both lasers exhibited similar light intensity / current (L-I) characteristics as the SOA current was ramped to 200 mA, with a maximum output of 40 mW. Referring to the individual lasers as L1 and L2, optical spectrum analyser (OSA) measurements showed tuning ranges of 8.4 nm (L1) and 8.7 nm (L2), decreasing from initial wavelengths of 1554.8 nm and 1560.7 nm for L1 and L2 respectively (Fig. 2). Due to the thermal coupling between the lasers, the temperature tuning of each laser was determined and found to follow a similar linear dependence of 13.2 – 13.6 GHz/ $^{\circ}\text{C}$ (Fig. 3), showing that due to their integration, the lasing peaks should track together, excepting for occasions of mode hopping.

Linewidth measurements were performed via heterodyning individual lasers with an external cavity laser (ECL) and by mixing the laser pair outputs together into a fast (15 GHz) InGaAs detector and monitoring the electrical beat noise spectrum on an RF electrical spectrum analyzer (ESA). Due to the sensitivity of the tuning to small current variations in the gratings, these measurements were performed with grating and phase sections shorted

whenever no tuning was necessary. Both of these methods yielded linewidths of around 15 MHz. Spectral characteristics of the devices were found to be stable while wavelength tuning indicating very low levels of coupling via facet reflections.

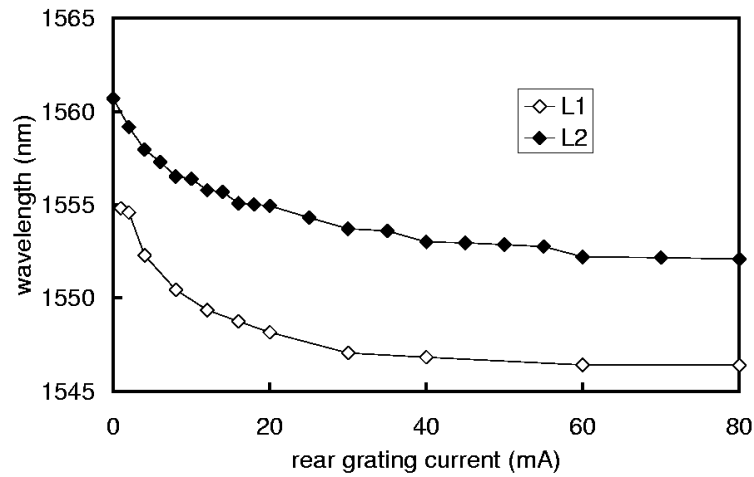


Fig. 2. Electrical tuning curves for the lasers showing lasing wavelength as a function of rear grating current.

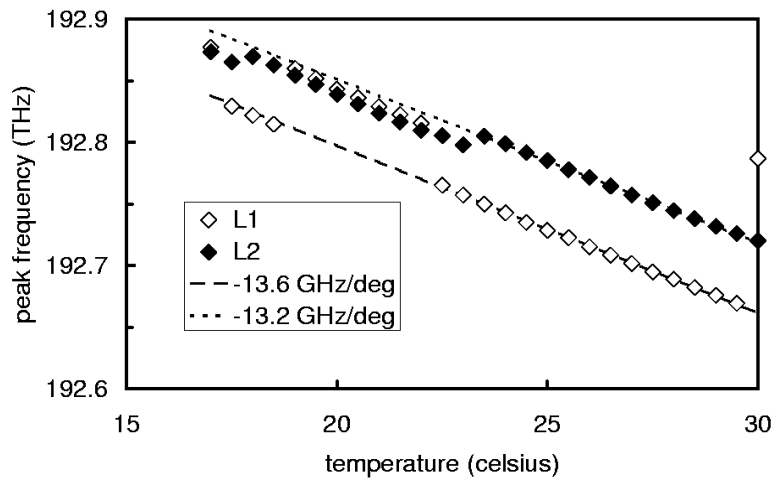


Fig. 3. Temperature tuning of the DBR lasers showing the peak lasing frequency as a function of temperature in celsius.

3. Experimental setup

For the mutual injection measurements, the device was mounted on a translation stage with a thermo-electric controller (TEC) and the output coupled into a cleave-ended fibre spliced to an optical isolator. The optical output was then distributed via couplers into the InGaAs detector / ESA system, an OSA and a scanning Fabry-Perot interferometer (FPI) (Fig. 4).

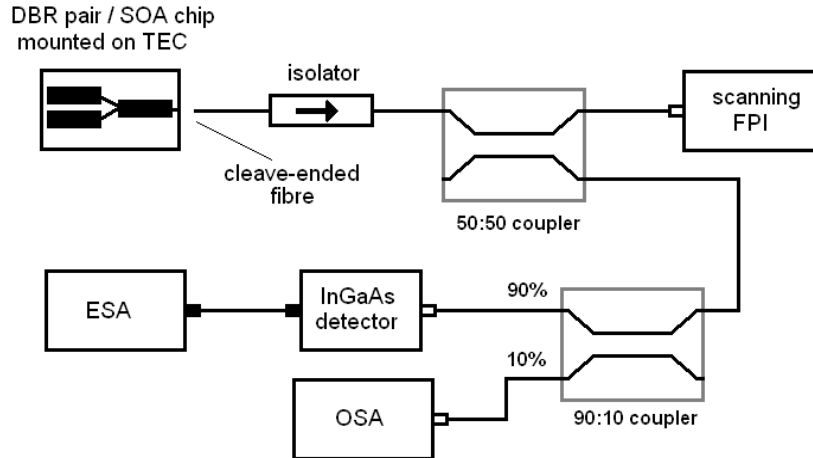


Fig. 4. Schematic of the experimental setup for the mutual injection measurements.

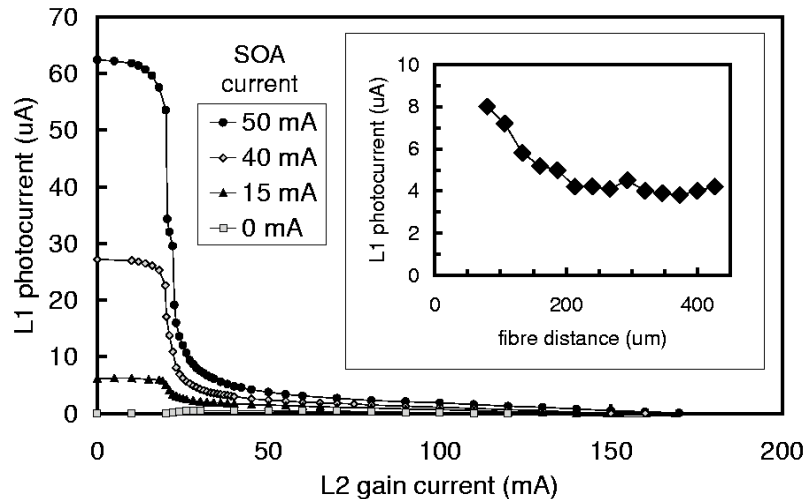


Fig. 5. Photocurrent in the L1 laser gain section as a function of L2 gain current and fibre distance with a gain and SOA currents of 60 mA and 30 mA respectively (insert).

In the measurement system the fibre performs the dual function of collecting the summed emission from the lasers and acting as reflector to couple light back into the laser pair. In order to assess the mutual coupling between the lasers via the level of reflection from the cleave-ended fibre, one of the laser gain sections can be used as a photodiode. Firstly with the fibre completely removed, Fig. 5 shows photocurrent in L1 when the gain current in L2 was increased from 0 to 200mA and with different values of SOA current. Beginning with L2 off (y axis), the resulting photocurrent measured with L1 biased as a photodiode was initially high due to amplified spontaneous emission (ASE) power generated in the SOA propagating back along the waveguide into the laser. However as the current in L2 is increased beyond threshold, a reduction in the photocurrent in L1 resulting from the suppression of ASE noise can clearly be seen as the SOA saturates. With the fibre placed to achieve high coupled power, additional photocurrent is observed in L1 due to the back reflection from the cleaved

fibre end. As the fibre is moved away from the device the photocurrent is seen to decrease, corresponding to weaker feedback (insert, Fig. 5). By measuring the difference between the photocurrent with and without the fibre, the relative strength of the optical coupling between the devices can be assessed and adjusted. The term ‘strong coupling’ will be used to refer to the case where the power into the fibre has been optimised with a typical distance from the cleave to the fibre of about 80 μm , and ‘weak coupling’ to the situation where the fibre has been moved to a distance greater than 400 μm (the actual distance will be specified in any particular case). The time of flight between facet and fibre end, being of the order of a picosecond or less, makes little significant contribution to the coupling time of 30ps.

To differentiate the effects of optical feedback into the individual lasers from mutual coupling, the lasers were operated both individually and at the same time. At low SOA powers ($< \sim 80$ mA drive current), the spectra for the individual lasers did not exhibit any nonlinear effects, although at higher powers nonlinear behaviour was observed. The proper analysis of this system will therefore require both consideration of optical feedback and nonlinear mixing in the SOA.

4. Nonlinear phenomena

With the DBR lasers tuned to oscillate sufficiently far apart i.e. beyond the locking bandwidth, the primary nonlinear phenomenon we would expect to see is four-wave mixing in the SOA [29, 30]. This is illustrated in Fig. 6(a) and Fig. 6(b) for SOA currents of 80 mA and 90 mA respectively in the strong coupling regime. The initial detuning between the lasers (i.e. the detuning between the lasers operating independently) was 87 GHz, although as the SOA current is ramped, both lasers exhibit a shift in lasing peak of -0.30 GHz/mA and -0.14 GHz/mA for L1 and L2 respectively, so that the peaks actually move together at a rate of 0.16 GHz/mA. The apparent increase in detuning shown in the graphs is due to a mode hop on L1 of ~ 50 GHz. Both graphs show clear evidence of four-wave mixing, with side modes appearing at frequencies displaced from the peaks by the detuning frequency. At 90 mA SOA current, the spectrum was observed to become slightly unstable with side modes appearing either side of the main peaks at 7 GHz separations, believed to be due to relaxation oscillations.

That the four-wave mixing is taking place in the SOA is evidenced by measurements taken in the weak coupling regime (with a distance to the fibre end of 600 μm). Figures 7(a) and 7(b) show spectra with an initial detuning (between the peaks of the independently operating lasers shown by the dashed lines) of 9 GHz and 18 GHz respectively. Again the spectra show side modes offset by the detuning frequency. Note that the initial detuning is maintained despite an SOA current of 43 mA. The main peaks are shifted down in frequency by 17 GHz in each case, suggesting that this is due to the thermal coupling between the lasers when both are on since they should track together when thermally tuned. The residual pulling between the peaks seen only in the strong coupling regime may therefore be attributed to an effect of the optical coupling. Such frequency pulling between modes in mutually coupled lasers in the short coupling regime has also been observed in refs [26, 27].

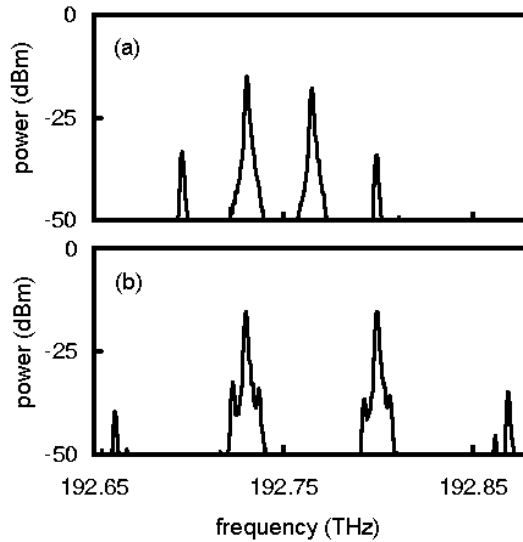


Fig. 6. OSA spectra with 80 mA (a) and 90 mA (b) SOA current.

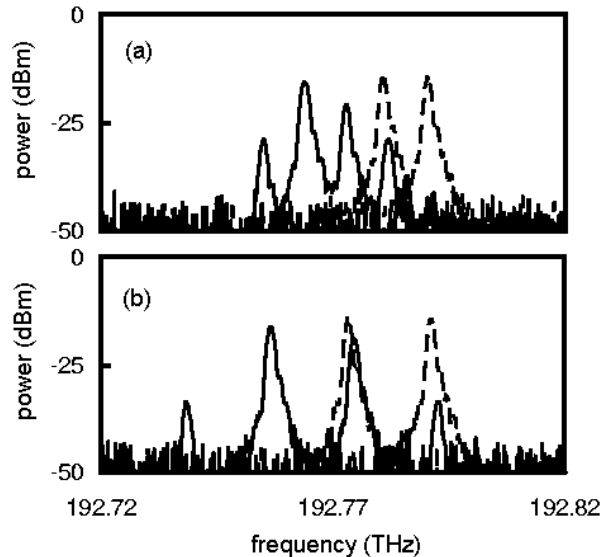


Fig. 7. OSA spectra with an initial detuning of 9 GHz (a) and 18 GHz (b) with 43 mA SOA current in the weak coupling regime (distance to fibre 600 μm). The dashed lines show the spectra of each laser operating alone.

At smaller detunings, a rich variety of nonlinear phenomena are observed characteristic of optical injection, including locking, period doubling and chaotic behaviour. With the lasing peaks initially close together (< 10 GHz), locking has been observed at low SOA powers, although occasionally an 'anti-locking' effect is seen when one or other of the lasers mode hops. At higher SOA powers, multi-mode and chaotic spectra are seen. Figure 8 shows a sequence of spectra in the strong coupling regime at different SOA powers where the lasers were initially mode locked. As the SOA current was ramped up, the spectra went through a sequence of two distinct modes (around 15 mA); chaotic behaviour (around 18 mA); broad multi-mode spectra (30 – 45 mA) and broad, fairly amorphous spectra spread over a range of

120 GHz (45 – 60 mA) with chaotic behaviour around 50 mA. From around 70 mA upwards, the amorphous spectra began to form the modal features seen in the last detail of Fig. 8, which have spacings of 3 to 9 GHz.

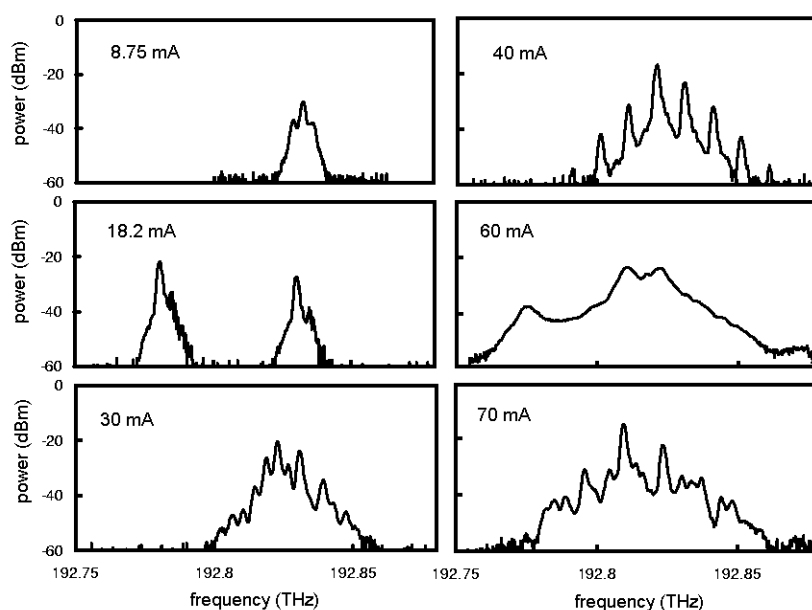


Fig. 8. OSA spectra in the strong coupling regime with an initial detuning of 0 GHz for 8.75 mA to 70 mA SOA current.

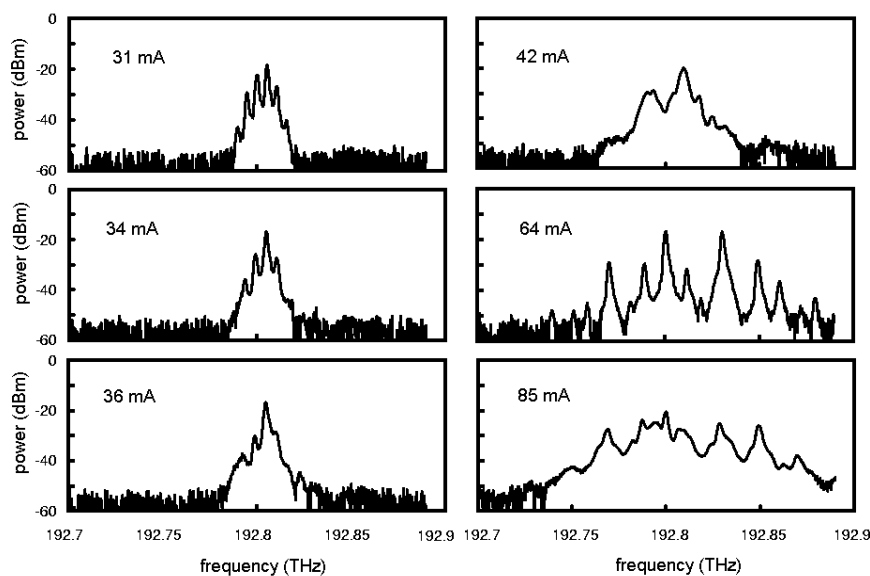


Fig. 9. OSA spectra in the strong coupling regime with an initial detuning of 7 GHz for 31 to 85 mA SOA current.

Figure 9 shows another sequence of spectra with increasing SOA power for an initial detuning of 7 GHz. In this case, the detuning is close to the frequency of the relaxation oscillations and the spectra at low SOA powers show distinct multi-modal patterns with

spacings of 5 – 6 GHz. Here, the presence of several peaks within around 20 dB of each other suggests that the phenomenon cannot be attributed solely to four-wave mixing but arises via the mutual coupling or a combination of both effects.

In Fig. 10, we see an example of a broad spectrum observed in the weak coupling regime (distance to fibre $\sim 430 \mu\text{m}$) with an initial detuning of 11 GHz and SOA current of 78 mA. Vague modal features may be discerned, suggesting that this may consist of broad peaks with 3 – 4 GHz spacings. In this case, the low coupling suggests that this is a phenomenon occurring in the SOA.

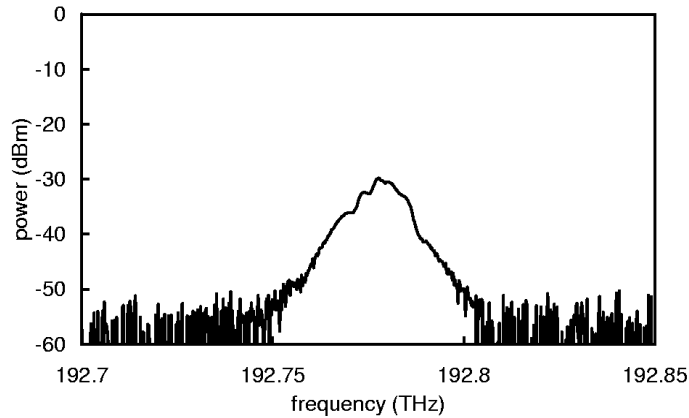


Fig. 10. OSA spectra with an initial detuning of 11 GHz with 78 mA SOA current in the weak coupling regime (distance to fibre $430 \mu\text{m}$).

5. Conclusions

We have reported experimental observations of a variety of nonlinear effects observed in a paired laser system, indicative of mutual coupling, optical feedback and nonlinear optical effects. A proper theoretical treatment of the system would need to account for the thermal coupling between the lasers, amplified mutual optical coupling, optical feedback strength and nonlinear effects in the SOA and has not, to our knowledge, been undertaken. Such phenomena may have important consequences for integrated optical systems and will be the subject of further investigation.

Acknowledgments

This work is funded by EPSRC grant EP/D502225/1.